Am J Transl Res 2024;16(12):8008-8022
www.ajtr.org /ISSN:1943-8141/AJTR0161111

Original Article

Determination of osimertinib concentration in rat plasma and lung/brain tissues

Yalan Zuo[1*], Peidan Yang[2*], Ruixia Yang[1], Juan Hou[1], Rui Feng[1], Ping Liang[1], Jiang Liu[1]

[1]Department of Pharmacy, The Fourth Hospital of Hebei Medical University, Shijiazhuang 050000, Hebei, China; [2]College of Pharmacy, Hebei Medical University, Shijiazhuang 050000, Hebei, China. [*]Equal contributors and co-first authors.

Received October 12, 2024; Accepted December 6, 2024; Epub December 15, 2024; Published December 30, 2024

Abstract: Objectives: The aim of this study was to establish an ultra-performance liquid chromatography-tandem mass spectrometry (UPLC-MS/MS) method for the detection of osimertinib in rat plasma, lung and brain tissues. Methods: Forty-eight rats were randomly divided into an experimental group (receiving osimertinib at doses of 5, 8, and 10 mg/kg) and a control group. After continuous intragastric administration for 15 days, samples of blood, lung, and brain tissue were collected. Chromatographic separation was achieved using a BEH C18 column with gradient elution, employing a mobile phase of water (containing 0.1% (v/v) formic acid) and acetonitrile. The concentration of osimertinib in the samples was determined using an AB SCIEX 5500 triple quadrupole mass spectrometer operated in positive electrospray ionization (ESI+) and multiple reaction monitoring (MRM) mode. Results: A UPLC-MS/MS analytical method for determining osimertinib concentrations was successfully established and validated. A linear relationship was observed for osimertinib concentrations in plasma within the range of 1-300 ng/mL, and in lung and brain tissues within the range of 0.5-50 ng/mL. The selectivity, accuracy, precision, matrix effect, extraction recovery, and stability all meet the requirements of methodological validation criteria. Conclusions: A rapid and sensitive UPLC-MS/MS method was developed and validated for quantifying osimertinib concentrations in rat plasma, lung, and brain tissues, providing a valuable tool for pharmacokinetic and tissue distribution studies.

Keywords: Osimertinib, EGFR-tyrosine kinase inhibitor, UPLC-MS/MS, concentration determination

Introduction

According to the World Health Organization, lung cancer has emerged as the leading cause of cancer-related deaths in recent years, both in China [1, 2] and globally [3]. Clinically, lung cancer is categorized into small-cell lung cancer (SCLC) and non-small cell lung cancer (NSCLC) [4, 5]. NSCLC accounts for approximately 85% of all lung cancer cases, with nearly 75% of patients diagnosed at the middle or late stages of the disease [6, 7]. Among these cases, 11%-60% of NSCLC patients harbor mutations in the human epidermal growth factor receptor (EGFR) gene [8, 9]. EGFR-tyrosine kinase inhibitors (EGFR-TKIs) are the current first-line standard treatment for advanced-stage NSCLC patients with EGFR mutations [10-12].

Osimertinib, a third-generation EGFR-TKI, has demonstrated potent inhibitory effects and central nervous system (CNS) therapeutic activity against EGFR mutations, including *T790M*, *Ex19del*, and *L858R* [13-15]. Due to its relatively small molecular weight and excellent lipid solubility, osimertinib can effectively cross the blood-brain barrier, enabling control of NSCLC brain metastases in patients with EGFR-positive mutations [13, 16]. In 2020, osimertinib was endorsed by both the National Comprehensive Cancer Network (NCCN) and the Chinese Society of Clinical Oncology (CSCO) guidelines as a first-line treatment for patients with advanced EGFR-mutant NSCLC [17, 18].

Currently, the primary methods for determining the concentration of EGFR-TKIs in samples include high-performance liquid chromatogra-

https://doi.org/10.62347/SYZD2489

phy (HPLC), HPLC-tandem mass spectrometry (HPLC-MS/MS), ultra-performance liquid chromatography-tandem mass spectrometry (UPLC-MS/MS), and other quantitative analytical techniques [19, 20]. Both HPLC and HPLC-MS/MS are commonly employed to measure the concentrations of osimertinib and its metabolites in plasma or tissue samples [21-23]. However, these methods are time-intensive, involve complex sample preparation procedures, and require relatively large sample volumes (100 μL), which limits their utility in pharmacokinetic studies [23]. In contrast, UPLC-MS/MS has been successfully applied to measure osimertinib concentrations in blood with improved efficiency [24-26]. Despite this, most quantitative studies of EGFR-TKIs have primarily focused on plasma samples [27, 28], with limited research addressing the simultaneous quantification of drug concentrations in both plasma and tissues [29].

In this study, we successfully developed and validated a UPLC-MS/MS assay for the simultaneous quantification of osimertinib in rat plasma, lung tissue, and brain tissue. Additionally, this method was effectively applied to investigate the pharmacokinetics of osimertinib in rats.

Materials and methods

Instrumentation

All experiments were conducted using the following equipment: an AB 5500 Triple Quadrupole Liquid Chromatograph-Mass Spectrometer (SCIEX Co., Ltd., Framingham, MA, USA); a TG16-WS Centrifuge (Changsha Xiangyi Centrifugal Instrument Co., Ltd., Changsha, China); an MS105 Micro Analytical Balance (Mettler Toledo Technology Co., Ltd., Shenzhen, China); a MIX-3000 Homogenizer (Hangzhou Mio Instrument Co., Ltd., Hangzhou, China); and a TJG-25 High-Throughput Ball Milling Instrument (Tianjin Dongfang Tiangyin Science and Technology Co., Ltd., Tianjin, China).

Drugs and reagents

Osimertinib mesylate standard (purity: 82.0%) and glimepiride (purity: 99.7%) were procured from the China Academy of Food and Drug Control. Osimertinib (batch no.: 2108506) was obtained from AstraZeneca Pharmaceutical Co., Ltd., London, United Kingdom. Methanol and acetonitrile (both of chromatographic grade) were supplied by Aladdin Reagent (Shanghai) Ltd., Shanghai, China. The 0.9% sodium chloride injection (250 mL) and 5% dextrose injection (250 mL) were purchased from Shijiazhuang Four Drugs Co., Ltd., Shijiazhuang, China.

Animals

Male Sprague-Dawley rats (n = 48, weight: 200 ± 20 g) were obtained from Stanford (Beijing) Biotechnology Co., Ltd. (Beijing, China; Animal Production License Number: SCXK (Beijing) 2019-0010). No other drugs were administered prior to the experiment, and the animals were acclimated for one week before testing. Prior to the experiment, the rats were fasted for 12 hours, with access to water but no food. During the testing period, the animals were kept in a quiet room under controlled conditions of temperature (15°C-25°C) and humidity (55%-65%). Outside of testing, they had free access to food and water. This study was approved by the Animal Centre of the Fourth Hospital of Hebei Medical University (Approval Number: 2023097).

Chromatographic conditions

A BEH C_{18} column (50 mm × 2.1 mm, 1.7 μm) was used for the analysis. The mobile phase consisted of 0.1% (v/v) formic acid aqueous solution (A) and acetonitrile (B), applied with a gradient elution as follows: 0.01-1.5 min, 20%-80% B; 1.5-4 min, 80% B; 4-4.1 min, 20%-80% B; 4.1-5 min, 20% B. The column temperature was maintained at 40°C, with a flow rate of 0.3 mL/min and an injection volume of 1 μL.

MS conditions

Electrospray ionization was conducted under the following conditions: positive ion mode with multiple reaction monitoring (MRM). The parameters were as follows: source voltage, 5,500 V; source temperature, 500°C; collision energy, 65 V; de-clustering voltage, 163 V; entrance voltage, 11 V; exit voltage, 15 V; nebulizing gas pressure, 55 psi; and heating assist gas pressure, 55 psi. The monitored transitions were osimertinib at *m/z* 500.2 → 72.1 and glimepiride at *m/z* 491.2 → 352.0.

Solution preparation

Preparation of standard solutions, calibration samples, and quality control (QC) samples: Osimertinib control product (3.07 mg) was accurately weighed, and an osimertinib reserve solution was prepared in 50% methanol at a concentration of 0.5 mg/mL. The stock solution was then accurately measured, and standard curve samples for rat plasma were prepared by diluting the stock solution to final concentrations of 1, 3, 10, 30, 50, 100, and 300 ng/mL. QC samples were prepared at concentrations of 1, 3, 30, and 240 ng/mL using the same method. Additionally, concentration gradient standard curve samples for brain and lung tissues were prepared at 0.5, 1, 3, 5, 10, 30, and 50 ng/mL, and QC samples were prepared at concentrations of 0.5, 1, 5, and 40 ng/mL.

Osimertinib solution: The osimertinib tablets were ground into fine powder. A measured amount of the powder was then weighed, dissolved in distilled water, vortexed, and mixed. The solution was subjected to ultrasonication until it was completely dispersed and transparent. Finally, the prepared solution was administered to the rats via gavage.

Internal standard solutions: Glimepiride (8.23 mg) was accurately weighed and dissolved in 50% (v/v) methanol to prepare a 1 mg/mL stock solution, which was then stored at -80°C. For concentration measurement, the stock solution was diluted with 50% (v/v) methanol to a final concentration of 100 ng/mL.

Sample handling methods

Rat plasma samples were retrieved from -80°C storage, thawed, and mixed at room temperature by vortexing. The samples were prepared using the methanol protein precipitation method. To each 1.5 mL plastic centrifuge tube, 20 μL of plasma sample was added, followed by 20 μL of internal standard solution (100 ng/mL glimepiride) and 100 μL of methanol. After vortex mixing (2,000 rpm for 2 min) and centrifugation (11,000 rpm for 5 min), the supernatant (30 μL) was collected. This supernatant was then diluted with 270 μL of 50% methanol, vortexed (2,000 rpm for 2 min), and analyzed by injection into a chromatography column. The data and chromatograms were recorded.

Brain and lung tissues were retrieved from the -80°C freezer, thawed at room temperature, and weighed. They were then supplemented with water at a 1:3 ratio and homogenized using a ball mill. The tissue samples were processed in the same manner as the plasma samples.

Selectivity: For plasma samples, selectivity was assessed by comparing the peak areas of six blank plasma samples, plasma samples from different rats treated with 1 ng/mL osimertinib, and plasma samples from rats administered osimertinib via gavage. This comparison aimed to determine whether any endogenous plasma components interfered with the detection of osimertinib.

For lung and brain tissues, selectivity was evaluated by comparing the peak areas of six blank tissue samples from different rats, tissue samples from rats treated with 0.5 ng/mL osimertinib, and tissue samples from rats administered osimertinib via gavage. This comparison helped identify whether any endogenous components in the lung and brain tissues interfered with the detection of osimertinib.

Residual effects: A standard curve and the QC plasma sample handling method, as described above, were used in this analysis. After injecting a plasma sample at the upper limit of quantification on the standard curve, a blank sample was also injected. The ratio of the peak area of osimertinib in the blank sample to that of the sample at the lower limit of quantification was calculated to assess the residual concentrations.

Standard curve and linear range: To generate a gradient standard curve, blank plasma was used to create seven serial 3-fold dilutions, ranging from 1 to 300 ng/mL. The samples were then injected into a chromatography column for analysis, and the peak areas were recorded. The concentration of osimertinib (on the *x*-axis) and the peak area ratios (on the *y*-axis) were weighted ($1/X^2$) using the least squares method for regression analysis, allowing the determination of the regression equation.

Accuracy and precision: Blank plasma was used to prepare osimertinib QC samples at different concentrations (1, 3, 30, and 240 ng/

mL) by diluting the working solution. Six parallel replicates of each QC concentration were prepared following the sample processing method described above, and the solutions were then injected into the chromatography column. Three consecutive analytical batches were analyzed to evaluate both intra-batch and inter-batch precision.

Matrix effects: Six blank rat plasma samples from different sources were used to prepare osimertinib QC samples at concentrations of 3 and 240 ng/mL, with six replicates prepared for each concentration. The peak areas of osimertinib (a) and glimepiride (b) were recorded following the sample processing method. Water was used to replace plasma, and the peak areas of osimertinib (A) and glimepiride (B) were recorded in the same manner. The matrix effect for both the substance to be measured and the internal standard was calculated by determining the ratio of the peak area in the presence of the matrix to the corresponding peak area without the matrix (a/A or b/B, respectively).

Extraction recovery: QC samples were prepared at three concentrations (3, 30, and 240 ng/mL), with six replicates of each concentration prepared in parallel, following the sample processing methods described previously. Additionally, a blank plasma sample was obtained from rats, and after protein precipitation, the supernatant was collected. The control QC solution of the substance to be measured and the internal standard solution were added to the supernatant. Six samples of each concentration were prepared in parallel and analyzed by UPLC-MS/MS.

Stability studies: Osimertinib QC samples were prepared at low and high concentrations (3 and 240 ng/mL, respectively) according to the standard blood sampling method previously described (six samples per QC concentration). The stability of osimertinib in simulated plasma samples was then evaluated under various conditions: at room temperature for 6 hours, in plasma samples stored at -80°C for 30 days, and after four freeze-thaw cycles. The concentration of the QC samples was analyzed according to the standard curve on the same day. The measured concentrations were required to be within ± 15% of the labeled concentration for relative error (RE), and the relative standard deviation (RSD) should be < 15%.

Dilution test: The drug concentration in lung tissues obtained from rats in the osimertinib group was within or above the assay range. To accurately measure the drug concentration in lung tissues, dilution experiments were performed using blank lung tissue. Specifically, the upper limit of quantification for the concentration in the samples was assessed by diluting the samples at a 3:5 ratio with lung tissue from blank rats (n = 6). If the RSD is ≤ 15%, the reliability of the dilution method is confirmed, ensuring that the dilutions used for the samples provide acceptable accuracy.

Pharmacokinetic studies

The Sprague-Dawley rats were randomly divided into a control group and an experimental group (5, 8, and 10 mg/kg) with 12 rats per group. The control and experimental groups were gavaged with distilled water and osimertinib (5, 8, and 10 mg/kg), respectively, once daily for 16 days. Blood samples (approximately 0.4 mL) were collected from the orbital region of the rats into ethylenediamine tetraacetic acid (EDTA) anticoagulant tubes at 0.5, 2, 4, 8, 12, and 24 hours following oral administration of osimertinib on days 1 and 15. At the end of the experiment, plasma samples, along with lung and brain tissues, were simultaneously collected. The rats were euthanized by intraperitoneal injection of 150 mg/kg pentobarbital sodium. Plasma was centrifuged at 3,000 rpm for 10 minutes at 4°C, and the supernatant was collected and stored at -80°C, along with the lung and brain tissues.

Results

Selectivity

Following UPLC-MS/MS analysis of osimertinib and glimepiride in plasma and tissues, the retention time was approximately 1.60 and 2.35 minutes, respectively (**Figure 1**). The results indicated that impurity components in the blood, lung, and brain tissue samples did not interfere with the detection of osimertinib.

Residual effects

A blank sample was injected after plasma samples at the upper limit of quantification of the standard curve (300 ng/mL). No residue of osimertinib was observed in the blank sample, and the ratio of the peak area of the internal

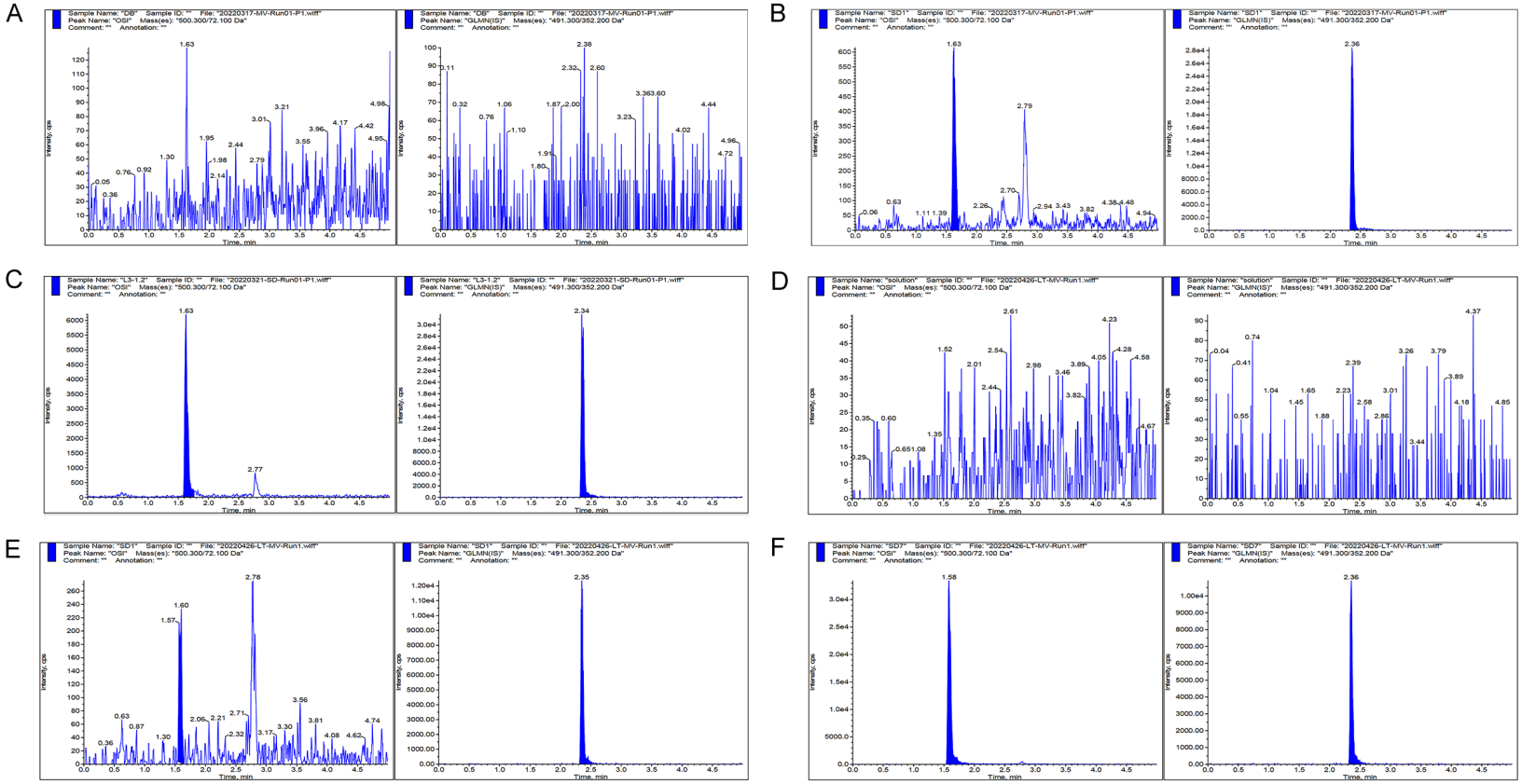
A
B
C
D
E
F

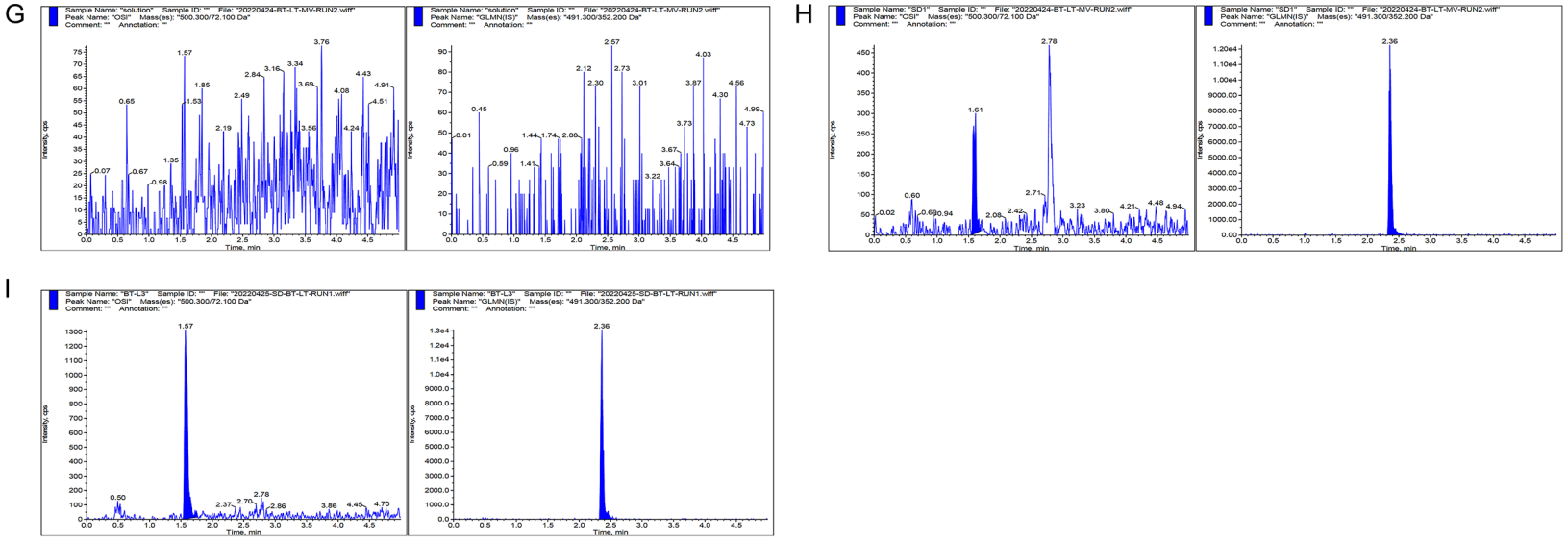

Figure 1. Typical chromatograms of osimertinib (left) and glimepiride (right). (A) Blank plasma and (B) blank plasma plus osimertinib 1 ng/mL and glimepiride 100 ng/Ml. (C) Plasma of the experimental group treated with 5 mg/kg gavage. (D) Blank lung tissue. (E) Blank lung tissue plus osimertinib 0.5 ng/mL and glimepiride 100 ng/mL. (F) Lung tissue of the experimental group treated with 5 mg/kg gavage. (G) Blank brain tissue. (H) Blank brain tissue plus osimertinib 0.5 ng/mL and glimepiride 100 ng/mL. (I) Brain tissue of the experimental group treated with 5 mg/kg gavage.

Table 1. Calibration range, typical calibration curve linear regression equation, and correlation coefficient (R^2) of osimertinib

Drug	Specimen	Linear range (ng/mL)	Standard curve	Correlation coefficient
Osimertinib	Blood	1-300	Y = 0.0297X+0.00192	0.9960
	Lungs, brain	0.5-50	Y = 0.696X-0.00114	0.9978

Table 2. Precision and accuracy of osimertinib in rat plasma (n = 6)

Batch	Precision (RSD%)	Accuracy (RE%)
Within a batch (except LLOQ)	5.90-12.30	-7.35 - -5.43
Within a batch (LLOQ)	9.16-12.10	-9.42-2.63
Between batches (except LLOQ)	6.19-11.90	-4.56 - -1.39
Between batches (LLOQ)	11.40	-3.38

LLOQ, lower limit of quantification; RE, relative error; RSD, relative standard deviation.

standard was 0.03%. These findings indicated that the residual effect did not impact the precision or accuracy of the assay.

Standard curves

The concentration of osimertinib (X) and the ratio of the peak area of osimertinib to the area of the internal standard, glimepiride (Y), were used as the horizontal and vertical coordinates, respectively. Linear regression was performed using the weighted least squares method ($1/X^2$) to obtain the regression equations for the standard curve of osimertinib (**Table 1**). The acceptance criteria were as follows: at least six of the concentrations had a RE ≤ 15%, and at least one of the lower or upper limits of quantification met the specified requirements.

Precision and accuracy

The lower limit of quantification (1 ng/mL) and the RSD of precision within and between batches for low (3 ng/mL), medium (30 ng/mL), and high (240 ng/mL) QC samples of osimertinib were ≤ 15%. The RE of accuracy within and between batches was ≤ 10%. The results demonstrated that the established UPLC-MS/MS method had good accuracy and high precision, meeting the requirements for method development and application. The specific results are shown in **Table 2**.

Matrix effects

The specific results for the peak area ratio of the QC samples and the internal standard, along with the osimertinib matrix effect factor, were calculated using six blank rat plasma samples obtained from different sources after treatment with osimertinib at low and high concentrations (3 and 240 ng/mL). These results are shown in **Table 3**. The preset criteria were met. The experimental results indicated that the matrix effect of osimertinib sample pretreatment in the rat plasma matrix complied with the pharmacopeial analytical method requirements.

Extraction recovery

The results of the extraction recoveries (**Table 4**) indicated that the average recoveries were 92.9% for osimertinib and 87.9% for glimepiride. These data demonstrate that the recoveries of the analytes using this method are high and stable, confirming the reliability of the analytical method.

Stability

The results of the osimertinib stability analysis are shown in **Table 5**. The precision of the samples was ≤ 15%, and the deviation of the average measured value from the theoretical value was ≤ ± 15%. These findings indicate that osimertinib remains stable in the short term, long term, and after multiple freeze-thaw cycles.

Titrations

The precision and accuracy were not affected by diluting the lung tissue samples at a 3:5 ratio in blank rat lung tissue, with an RSD of 7.34% and an RE of 2.52%. These findings confirm that the dilution method was reliable, and the dilutions used for the samples provided an acceptable level of accuracy.

Measurement of osimertinib concentrations in rats

We established and validated a UPLC-MS/MS method to determine the concentration of

Table 3. Matrix effect of osimertinib in rat plasma (n = 6)

Matrix effect %	LQC (3 ng/mL)	HQC (240 ng/mL)
Peak area ratio mean value of the substance to be measured	92.30	96.40
Mean internal standard peak area ratio	104.00	107.00
Mean values of internal standard normalized matrix effectors	90.40	87.30

HQC, high-quality control; LQC, low-quality control.

Table 4. Recovery for osimertinib in rat samples (n = 6)

Extraction recovery rate	Peak area after extraction			Unextracted peak area			Glimepiride	Undrawn
	LQC	MQC	HQC	LQC	MQC	HQC	Post-extraction	
Mean	4853	50967	355333	5802	50667	376667	58300	66322
SD	678	7369	44433	653	1861	21888	2291	9807
RSD (%)	14.00	14.50	12.50	11.30	3.70	5.80	3.93	14.80
Average recovery rate (%)	83.70	101.00	94.30		NA		87.90	NA
Overall recovery rate (%)			92.90				NA	NA
Overall variation CV (%)			10.30				NA	NA

CV, coefficient of variation; HQC, high-quality control; LQC, low-quality control; MQC, medium-quality control; NA, not applicable; RSD, relative standard deviation; SD, standard deviation.

Table 5. Stability of osimertinib (n = 6)

Prerequisite		LQC (3 ng/mL)			HQC (240 ng/mL)		
		RSD%	RE%	Mean	RSD%	RE%	Mean
Plasma placed for 6 h	25°C	2.76	12.40	-7.89	237.00	9.28	-1.12
Plasma placed for 30 days	-80°C	2.91	10.30	-2.73	253.00	6.77	5.63
Plasma freeze-thaw cycle (×4)	-80°C	2.97	4.91	-1.12	264.00	4.53	10.30

HQC, high-quality control; LQC, low-quality control; RE, relative error; RSD, relative standard deviation.

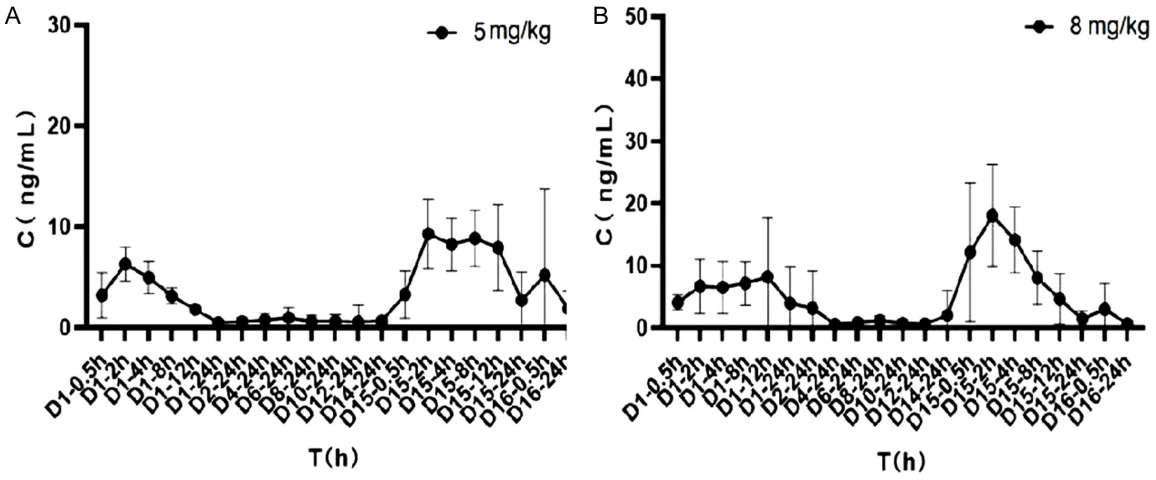

Figure 2. Plasma mean drug-time curves of 5 and 8 mg/kg experimental groups. A: 5 mg/kg. B: 8 mg/kg.

osimertinib in rats, using glimepiride as the internal standard. The blood concentration-time curves of osimertinib in the 5 and 8 mg/kg experimental groups are shown in **Figure 2**, while the curve for the 10 mg/kg experimental group is shown in **Figure 3**. In rat No. 2 of the 8 mg/kg group, parenchymal brain hemorrhage was observed, and its blood concentration-time curve is shown in **Figure 4**. Additionally, we determined the concentration of osimertinib in

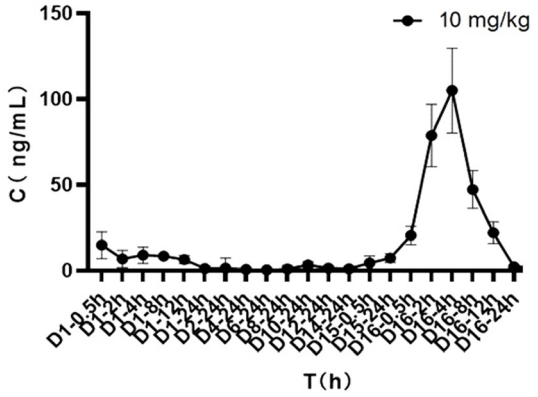

Figure 3. Plasma mean drug-time curve of the 10 mg/kg experimental group.

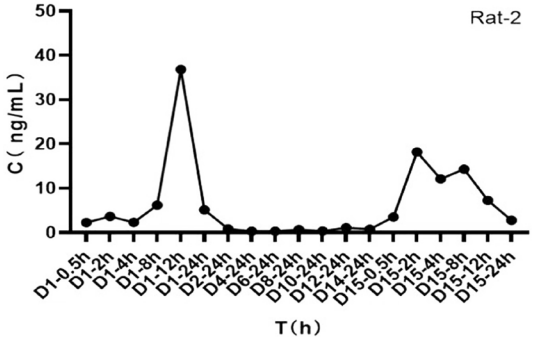

Figure 4. Plasma drug-time curve of a rat with cerebral hemorrhage.

the lung and brain tissues of rats using the same UPLC-MS/MS method (**Figure 5**), and the concentrations of osimertinib in these tissues are presented below. **Figures 2** and **3** demonstrate that the median time to reach the highest blood concentration of osimertinib was 3.3 h on day 15 across the three administered doses (5 mg/kg, 8 mg/kg, and 10 mg/kg). **Figure 4** shows that the cerebral hemorrhage did not affect the time to reach the peak concentration of osimertinib. As shown in **Figures 2**-**5**, the concentrations varied significantly in plasma, lung tissue, and brain tissue, with the highest concentrations in lung tissue, followed by plasma, and the lowest concentrations in brain tissue.

Pharmacokinetic studies

Pharmacokinetic analysis was performed using Phoenix WinNonlin 6.4 (Certara, Princeton, NJ, USA). The relevant pharmacokinetic parameters (**Table 6**) were analyzed for the different administered doses (5, 8, and 10 mg/kg). The time kurtosis ratios R_{cmax} (R_{cmax} = d15 C_{max}/d1 C_{max}) were 1.77, 1.65, and 1.70, respectively. These results indicate a certain degree of drug accumulation in the rats from the experimental groups. Dose-response curves were plotted using the log-transformed values of the administered dose (*X*) and C_{max} (*Y*) as the x- and y-axes, respectively. For the D1 dose-response curve, the equation was *Y* = 35.31*X*-18.33, and for the d15 dose-response curve, it was *Y* = 58.11*X*-29.55. The slopes of these curves were greater than 1, suggesting that osimertinib concentrations increase in a dose-dependent and proportional manner when administered at doses of 5-10 mg/kg.

Discussion

In this study, we optimized a UPLC-MS/MS method for determining osimertinib concentrations in plasma, lung, and brain tissues. During the preliminary stage, we investigated the effects of different elution gradients and mobile phase additives on the peak shapes, retention times, and response values of osimertinib and glimepiride. The optimized method provided faster chromatographic analyses while ensuring good separation by adding 0.1% (v/v) formic acid to the mobile phase. In optimizing the MS conditions, we found that osimertinib exhibited a higher response in the positive ion mode, with the monitoring ion pair determined as m/z: 500.2 → 72.1. Additionally, we selected a protein precipitation method for sample pretreatment. Methanol was chosen as the protein precipitation agent due to its simplicity, speed, cost-effectiveness, and minimal environmental impact [30]. This method provided an efficient, sensitive, and accurate approach for the quantitative analysis of osimertinib. Furthermore, the optimized method was successfully applied to a pharmacokinetic study of drug-drug interactions following oral administration of osimertinib in rats.

The rats in the experimental groups exhibited significant individual variability after drug administration. Additionally, more severe adverse reactions were observed, with the measured drug concentrations being lower in these rats. This led to considerable differences in drug concentrations across biological samples [31].

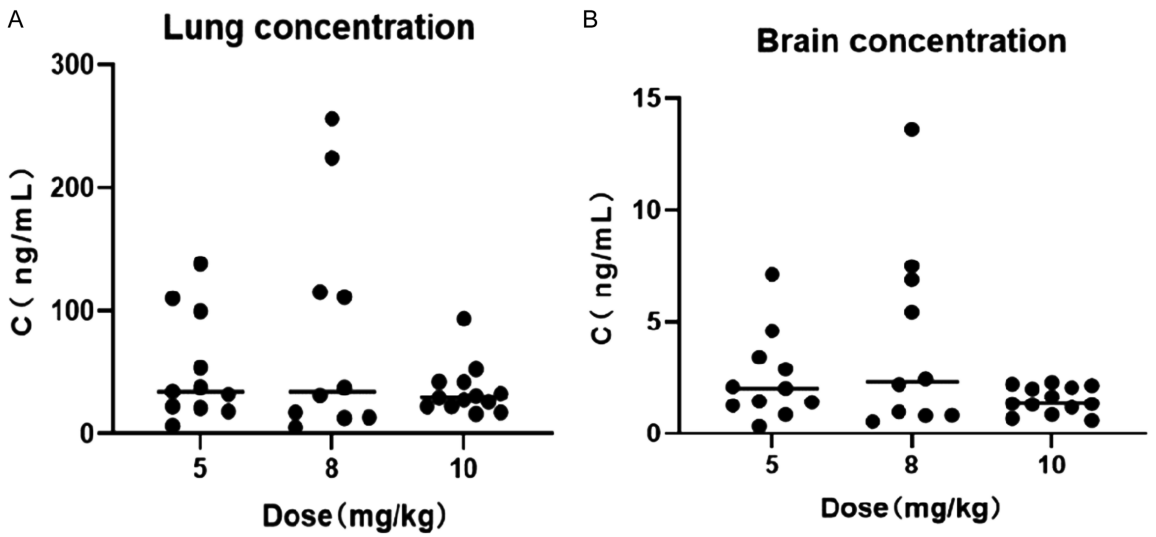

Figure 5. Concentrations of osimertinib in the lungs and brain. A: lung concentration. B: Brain concentration.

The concentration of osimertinib in rat plasma in our study was lower than that reported in other studies. For instance, Xiong et al. [23] reported a C_{max} of approximately 20 ng/mL for osimertinib in rats at a dose of 4.5 mg/kg, while Ying et al. [19] observed a C_{max} of about 300 ng/mL at a dose of 10 mg/kg. One possible explanation for this discrepancy is that the rats experienced gastrointestinal side effects, such as vomiting and diarrhea, due to the anesthesia used during the experiment [32]. In our study, chloral hydrate was employed as the anesthetic. This agent is known to be corrosive to the skin and mucous membranes and can significantly impact the gastrointestinal tract, which likely reduced drug absorption and contributed to the lower-than-expected concentration. Additionally, individual variations among the animals could also have influenced the concentration of the drug in their bodies [33].

In line with the study by Dong et al. [24], we found that rats could tolerate the usual dose of osimertinib (4.5-10 mg/kg). Based on this, we selected doses of 5, 8, and 10 mg/kg for our study. Additionally, gastrointestinal absorption of osimertinib appears to be relatively complete and stable within the 5-10 mg/kg dose range. This suggests that the proportion of the administered dose that reaches systemic circulation (bioavailability) does not change significantly as the dose increases [34]. Moreover, the metabolic and clearance pathways for osimertinib likely remain unaffected and unsaturated within this dose range [35], resulting in consistent elimination rate constants ($t_{1/2}$) across doses.

It is possible that osimertinib distribution in lung and brain tissue may not directly reflect the dose-proportional kinetics observed in the systemic circulation [36]. At the doses tested (5-10 mg/kg), distribution mechanisms in lung and brain tissue may become saturated, leading to a plateau or a non-linear relationship between the administered dose and tissue concentrations. Furthermore, tissue concentrations in this study were assessed after 15 days of continuous dosing. The absence of a dose-dependent trend may be related to the specific time point chosen for sample collection, and differences in concentrations may occur at earlier or later stages of the treatment course [37]. Consequently, future studies should consider investigating the time course of osimertinib concentrations in lung and brain tissue, potentially incorporating additional dose levels and sampling time points.

After dosing, the rats experienced severe gastrointestinal reactions such as nausea, vomiting, and diarrhea on day 1. However, by day 15, the rats no longer exhibited any gastrointestinal symptoms, leading to differences in peak times between day 1 and day 15. The peak time on day 15 was more reliable, with a median peak time of 3.3 hours across the different doses. A comparison of plasma, lung tissue,

Table 6. Pharmacokinetic parameters of osimertinib treatment groups in plasma from rats

PK parameters	5 mg/kg group		8 mg/kg group		10 mg/kg group	
	Day 1	Day 15	Day 1	Day 15	Day 1	Day 15
T_{max} (h)	2.16 ± 0.57	4.59 ± 3.74	7.70 ± 6.60	2.10 ± 1.17	2.25 ± 2.35	4.16 ± 1.33
C_{max} (ng/mL)	6.38 ± 1.61	11.30 ± 3.08	13.48 ± 8.79	22.21 ± 9.79	17.04 ± 5.91	29.05 ± 24.95
Lambda_z (1/h)	0.13 ± 0.03	0.11 ± 0.06	0.09 ± 0.04	0.15 ± 0.03	0.11 ± 0.05	0.19 ± 0.02
HL-lambda-z (h)	5.79 ± 1.90	8.08 ± 5.43	9.88 ± 5.62	4.85 ± 1.32	10.55 ± 11.92	3.69 ± 0.51
AUClast (h* ng/mL)	53.27 ± 17.57	138.86 ± 33.75	154.00 ± 82.10	154.26 ± 69.10	150.30 ± 31.59	325.92 ± 119.59
AUCINF_obs (h* ng/mL)	61.91 ± 13.78	166.65 ± 44.26	130.08 ± 34.04	178.61 ± 73.12	201.80 ± 99.18	289.06 ± 213.19
Vz_F_obs (mL/kg)	706272.70 ± 273938.6	333970.80 ± 174740.10	973791.20 ± 721293.20	337653.50 ± 88018.61	604263.10 ± 406889.40	240891.46 ± 103649.62
Cl_F_obs (mL/h/kg)	85203.27 ± 22638.54	32430.84 ± 10903.24	64897.77 ± 15827.57	51841.99 ± 20837.96	54110.48 ± 31456.86	45827.84 ± 19590.57
MRTINF_obs (h)	8.96 ± 2.39	13.56 ± 7.55	14.98 ± 7.87	7.50 ± 2.64	15.39 ± 16.31	7.43 ± 0.94

and brain tissue concentrations at various doses revealed a broad distribution of osimertinib, with the highest concentrations observed in lung tissue. This supports the notion that osimertinib is particularly effective in treating EGFR-mutated non-small-cell lung cancer compared to other solid tumors. Previous studies have indicated that osimertinib, a third-generation EGFR-TKI, has enhanced efficacy over first- and second-generation EGFR inhibitors [38]. However, this increased efficacy is accompanied by a notable rise in the incidence of adverse drug reactions (ADRs). ADRs can occur within a range of 2 days to 1 year following drug administration, with most adverse reactions happening between 1 week and 1 month after treatment initiation [39]. These reactions can affect multiple systems, including the respiratory, digestive, blood, cardiovascular, urinary, skin, and ocular systems, with approximately 65% of ADRs involving the respiratory and digestive systems [40]. Notably, there have been reports of patients experiencing respiratory-related adverse reactions, and in some cases, the discontinuation of osimertinib has led to rapid cancer progression and patient death [41, 42]. In this study, we observed that some rats exhibited significantly higher drug concentrations in the lungs or brain compared to others and displayed signs of irritability. One rat in the 8 mg/kg experimental group developed parenchymal hemorrhage, and its blood concentration of osimertinib was higher than that of the other rats in the same group. It has been reported that osimertinib can cause neurotoxic adverse reactions, so the irritability and other behavioral changes in the rats may be related to the drug. Autopsy results revealed that half of the rats in the experimental groups had severe lung damage. This suggests a potential link between drug concentrations in brain tissue and changes in mental state, as well as a relationship between drug concentrations in lung tissue and lung injury. However, there is currently no available research to support this hypothesis, and further studies are needed to explore these potential correlations.

Monitoring osimertinib concentrations in rat plasma is crucial for identifying resistance mechanisms, particularly after the progression of osimertinib treatment. This approach is essential for prolonging patient survival and improving quality of life. Studies on the pharmacokinetics of osimertinib, especially in rat models, provide valuable insights into drug absorption, distribution, metabolism, and excretion, which are fundamental for optimizing drug administration strategies and enhancing therapeutic efficacy. The determination of osimertinib concentration in plasma and cerebrospinal fluid using ultra-high-performance liquid chromatography (UPLC) offers high sensitivity, strong anti-interference capability, and excellent stability, making it an ideal method for monitoring osimertinib concentrations in blood. The establishment and application of this method provides a rapid, simple, cost-effective, and practical means of blood drug concentration detection for clinical practice. This approach supports individualized treatment and therapeutic drug monitoring. Therefore, blood concentration monitoring and pharmacokinetic studies of osimertinib in rats are highly significant for understanding drug behavior in vivo, optimizing treatment regimens, predicting human responses, and supporting drug development and approval.

Osimertinib is a third-generation EGFR-TKI widely used in the treatment of NSCLC. Compared with previous pharmacokinetic studies of osimertinib, the present study offers a deeper understanding of the drug's distribution and metabolism across different tissues by determining its concentration in rat plasma, lung, and brain tissues. Additionally, osimertinib has central nervous system activity, making the measurement of its concentration in brain tissue crucial for evaluating its efficacy against brain metastases. This study demonstrated that osimertinib is capable of crossing the blood-brain barrier and was detected at measurable concentrations in brain tissue, providing important insights into its distribution within the CNS. The pharmacokinetic properties of osimertinib in various tissues also help elucidate its resistance mechanisms and offer a theoretical foundation for strategies to overcome drug resistance. However, while the rat model offers valuable preliminary pharmacokinetic data, its findings may not fully translate to human pharmacokinetics. Therefore, further research is needed to establish the population pharmacokinetics of osimertinib in humans, particularly in plasma and cerebrospinal fluid, to address this critical gap.

Adverse reactions to osimertinib can affect multiple organs, highlighting the importance of

clinical monitoring to reduce the incidence of side effects and ensure patient safety [43]. In this study, we established and validated a UPLC-MS/MS method for the rapid, accurate, and sensitive detection of osimertinib concentrations in rats. This method provides valuable insights into the pharmacokinetics of osimertinib and may serve as a useful tool for future research and clinical applications, ultimately guiding treatment decisions and improving patient outcomes.

Conclusion

A sensitive, simple, and cost-effective UPLC-MS/MS method was developed for the simultaneous determination of osimertinib concentrations in rat plasma and tissues. The method was thoroughly validated to meet all regulatory requirements for selectivity, sensitivity, linearity, accuracy, precision, and stability. As a result, this method holds great potential as a key tool to support clinical practice, including therapeutic drug monitoring and pharmacokinetic studies of analytes, ultimately enhancing treatment outcomes and providing valuable insights into drug behavior.

Acknowledgements

The authors of this work would like to acknowledge the financial support offered by The Fourth of Hebei Medical University Researchers Supporting Project number (H2021206441), Hebei Medical University.

Disclosure of conflict of interest

None.

Address correspondence to: Ping Liang and Jiang Liu, Department of Pharmacy, The Fourth Hospital of Hebei Medical University, No. 12 Jiankang Road, Chang'an District, Shijiazhuang 050000, Hebei, China. E-mail: 48001098@hebmu.edu.cn (PL); 46500785@hebmu.edu.cn (JL)

References

[1] Dingemans AC, Soo RA, Jazieh AR, Rice SJ, Kim YT, Teo LLS, Warren GW, Xiao SY, Smit EF, Aerts JG, Yoon SH, Veronesi G, De Cobelli F, Ramalingam SS, Garassino MC, Wynes MW, Behera M, Haanen J, Lu S, Peters S, Ahn MJ, Scagliotti GV, Adjei AA and Belani CP. Treatment guidance for patients with lung cancer during the coronavirus 2019 pandemic. J Thorac Oncol 2020; 15: 1119-1136.

[2] Chen W, Zhang S and Zou X. Evaluation on the incidence, mortality and tendency of lung cancer in China. Thorac Cancer 2010; 1: 35-40.

[3] Schenk EL, Patil T, Pacheco J and Bunn PA Jr. 2020 innovation-based optimism for lung cancer outcomes. Oncologist 2021; 26: e454-e472.

[4] Oser MG, Niederst MJ, Sequist LV and Engelman JA. Transformation from non-small-cell lung cancer to small-cell lung cancer: molecular drivers and cells of origin. Lancet Oncol 2015; 16: e165-e172.

[5] Gridelli C, Rossi A, Carbone DP, Guarize J, Karachaliou N, Mok T, Petrella F, Spaggiari L and Rosell R. Non-small-cell lung cancer. Nat Rev Dis Primers 2015; 1: 15009.

[6] Cao W, Chen HD, Yu YW, Li N and Chen WQ. Changing profiles of cancer burden worldwide and in China: a secondary analysis of the global cancer statistics 2020. Chin Med J (Engl) 2021; 134: 783-791.

[7] Schabath MB and Cote ML. Cancer progress and priorities: lung cancer. Cancer Epidemiol Biomarkers Prev 2019; 28: 1563-1579.

[8] Melosky B, Kambartel K, Häntschel M, Bennetts M, Nickens DJ, Brinkmann J, Kayser A, Moran M and Cappuzzo F. Worldwide prevalence of epidermal growth factor receptor mutations in non-small cell lung cancer: a meta-analysis. Mol Diagn Ther 2022; 26: 7-18.

[9] Jorge SE, Kobayashi SS and Costa DB. Epidermal growth factor receptor (EGFR) mutations in lung cancer: preclinical and clinical data. Braz J Med Biol Res 2014; 47: 929-939.

[10] Greenhalgh J, Boland A, Bates V, Vecchio F, Dundar Y, Chaplin M and Green JA. First-line treatment of advanced epidermal growth factor receptor (EGFR) mutation positive non-squamous non-small cell lung cancer. Cochrane Database Syst Rev 2021; 3: CD010383.

[11] Sullivan I and Planchard D. Next-generation EGFR tyrosine kinase inhibitors for treating EGFR-mutant lung cancer beyond first line. Front Med (Lausanne) 2017; 3: 76.

[12] Nan X, Xie C, Yu X and Liu J. EGFR TKI as first-line treatment for patients with advanced EGFR mutation-positive non-small-cell lung cancer. Oncotarget 2017; 8: 75712-75726.

[13] Gen S, Tanaka I, Morise M, Koyama J, Kodama Y, Matsui A, Miyazawa A, Hase T, Hibino Y, Yokoyama T, Kimura T, Yoshida N, Sato M and Hashimoto N. Clinical efficacy of osimertinib in EGFR-mutant non-small cell lung cancer with distant metastasis. BMC Cancer 2022; 22: 654.

[14] Wu L, Ke L, Zhang Z, Yu J and Meng X. Development of EGFR TKIs and options to manage resistance of third-generation EGFR TKI osimertinib: conventional ways and immune checkpoint inhibitors. Front Oncol 2020; 10: 602762.
[15] Tan CS, Kumarakulasinghe NB, Huang YQ, Ang YLE, Choo JR, Goh BC and Soo RA. Third generation EGFR TKIs: current data and future directions. Mol Cancer 2018; 17: 29.
[16] Economopoulou P and Mountzios G. Non-small cell lung cancer (NSCLC) and central nervous system (CNS) metastases: role of tyrosine kinase inhibitors (TKIs) and evidence in favor or against their use with concurrent cranial radiotherapy. Transl Lung Cancer Res 2016; 5: 588-598.
[17] Lv C, Fang W, Wu N, Jiao W, Xu S, Ma H, Wang J, Wang R, Ji C, Li S, Wang Y, Yan S, Lu F, Pei Y, Liu Y and Yang Y. Osimertinib as neoadjuvant therapy in patients with EGFR-mutant resectable stage II-IIIB lung adenocarcinoma (NEOS): a multicenter, single-arm, open-label phase 2b trial. Lung Cancer 2023; 178: 151-156.
[18] Nagasaka M, Zhu VW, Lim SM, Greco M, Wu F and Ou SI. Beyond osimertinib: the development of third-generation EGFR tyrosine kinase inhibitors for advanced EGFR+ NSCLC. J Thorac Oncol 2021; 16: 740-763.
[19] Ying Z, Wei J, Liu R, Zhao F, Yu Y and Tian X. An UPLC-MS/MS method for determination of osimertinib in rat plasma: application to investigating the effect of ginsenoside Rg3 on the pharmacokinetics of osimertinib. Int J Anal Chem 2020; 2020: 8814214.
[20] Xing L, Pan Y, Shi Y, Shu Y, Feng J, Li W, Cao L, Wang L, Gu W, Song Y, Xing P, Liu Y, Gao W, Cui J, Hu N, Li R, Bao H, Shao Y and Yu J. Biomarkers of osimertinib response in patients with refractory, EGFR-T790M-positive non-small cell lung cancer and central nervous system metastases: the APOLLO study. Clin Cancer Res 2020; 26: 6168-6175.
[21] Rood JJM, van Haren MJ, Beijnen JH and Sparidans RW. Bioanalysis of EGFRm inhibitor osimertinib, and its glutathione cycle- and desmethyl metabolites by liquid chromatography-tandem mass spectrometry. J Pharm Biomed Anal 2020; 177: 112871.
[22] Aghai-Trommeschlaeger F, Zimmermann S, Gesierich A, Kalogirou C, Goebeler ME, Jung P, Pelzer T, Kurlbaum M, Klinker H, Isberner N and Scherf-Clavel O. Comparison of a newly developed high performance liquid chromatography method with diode array detection to a liquid chromatography tandem mass spectrometry method for the quantification of cabozantinib, dabrafenib, nilotinib and osimertinib in human serum - application to therapeutic drug monitoring. Clin Biochem 2022; 105-106: 35-43.
[23] Xiong S, Deng Z, Sun P, Mu Y and Xue M. Development and validation of a rapid and sensitive LC-MS/MS method for the pharmacokinetic study of osimertinib in rats. J AOAC Int 2017; 100: 1771-1775.
[24] Dong ST, Li Y, Yang HT, Wu Y, Li YJ, Ding CY, Meng L, Dong ZJ and Zhang Y. An accurate and effective method for measuring osimertinib by UPLC-TOF-MS and its pharmacokinetic study in rats. Molecules 2018; 23: 2894.
[25] Zheng X, Wang W, Zhang Y, Ma Y, Zhao H, Hu P and Jiang J. Development and validation of a UPLC-MS/MS method for quantification of osimertinib (AZD9291) and its metabolite AZ5104 in human plasma. Biomed Chromatogr 2018; 32: e4365.
[26] Xu Y, Qie H, Zhao H, Gao X, Gao J, Feng Z, Bai J and Wang M. Simultaneous determination of icotinib, osimertinib, aumolertinib, and anlotinib in human plasma for therapeutic drug monitoring by UPLC-MS/MS. J Pharm Biomed Anal 2024; 251: 116445.
[27] Solassol I, Pinguet F and Quantin X. FDA- and EMA-approved tyrosine kinase inhibitors in advanced EGFR-Mutated non-small cell lung cancer: safety, tolerability, plasma concentration monitoring, and management. Biomolecules 2019; 9: 668.
[28] Sun W, Yuan X, Tian Y, Wu H, Xu H, Hu G and Wu K. Non-invasive approaches to monitor EGFR-TKI treatment in non-small-cell lung cancer. J Hematol Oncol 2015; 8: 95.
[29] Gammelgaard B, Hansen HR, Stürup S and Møller C. The use of inductively coupled plasma mass spectrometry as a detector in drug metabolism studies. Expert Opin Drug Metab Toxicol 2008; 4: 1187-1207.
[30] Fang Z, Zhang H, Guo J and Guo J. Overview of therapeutic drug monitoring and clinical practice. Talanta 2024; 266: 124996.
[31] Lindon JC, Holmes E, Bollard ME, Stanley EG and Nicholson JK. Metabonomics technologies and their applications in physiological monitoring, drug safety assessment and disease diagnosis. Biomarkers 2004; 9: 1-31.
[32] Zhong W, Shahbaz O, Teskey G, Beever A, Kachour N, Venketaraman V and Darmani NA. Mechanisms of nausea and vomiting: current knowledge and recent advances in intracellular emetic signaling systems. Int J Mol Sci 2021; 22: 5797.
[33] Martinez MN. Factors influencing the use and interpretation of animal models in the development of parenteral drug delivery systems. AAPS J 2011; 13: 632-649.
[34] Fujiwara Y, Makihara R, Hase T, Hashimoto N, Naito T, Tsubata Y, Okuno T, Takahashi T, Ko-

bayashi H, Shinno Y, Zenke Y, Ikeda T, Hosomi Y, Watanabe K, Kitazono S, Sakiyama N, Makino Y and Yamamoto N. Pharmacokinetic and dose-finding study of osimertinib in patients with impaired renal function and low body weight. Cancer Sci 2023; 114: 2087-2097.

[35] Rodier T, Puszkiel A, Cardoso E, Balakirouchenane D, Narjoz C, Arrondeau J, Fallet V, Khoudour N, Guidi M, Vidal M, Declèves X, Csajka C, Alexandre J, Cadranel J, Fabre E, Wislez M, Goldwasser F and Blanchet B. Exposure-response analysis of osimertinib in patients with advanced non-small-cell lung cancer. Pharmaceutics 2022; 14: 1844.

[36] Teicher BA and Morris J. Antibody-drug conjugate targets, drugs, and linkers. Curr Cancer Drug Targets 2022; 22: 463-529.

[37] Tyson RJ, Park CC, Powell JR, Patterson JH, Weiner D, Watkins PB and Gonzalez D. Precision dosing priority criteria: drug, disease, and patient population variables. Front Pharmacol 2020; 11: 420.

[38] Takeda M and Nakagawa K. First- and second-generation EGFR-TKIs are all replaced to osimertinib in chemo-naive EGFR mutation-positive non-small cell lung cancer? Int J Mol Sci 2019; 20: 146.

[39] Miguel A, Azevedo LF, Araújo M and Pereira AC. Frequency of adverse drug reactions in hospitalized patients: a systematic review and meta-analysis. Pharmacoepidemiol Drug Saf 2012; 21: 1139-1154.

[40] Anand K, Ensor J, Trachtenberg B and Bernicker EH. Osimertinib-induced cardiotoxicity: a retrospective review of the fda adverse events reporting system (FAERS). JACC CardioOncol 2019; 1: 172-178.

[41] Steinberg KP, Hudson LD, Goodman RB, Hough CL, Lanken PN, Hyzy R, Thompson BT and Ancukiewicz M; National Heart, Lung, and Blood Institute Acute Respiratory Distress Syndrome (ARDS) Clinical Trials Network. Efficacy and safety of corticosteroids for persistent acute respiratory distress syndrome. N Engl J Med 2006; 354: 1671-1684.

[42] Takakuwa O, Oguri T, Uemura T, Sone K, Fukuda S, Okayama M, Kanemitsu Y, Ohkubo H, Takemura M, Ito Y, Maeno K and Niimi A. Osimertinib-induced interstitial lung disease in a patient with non-small cell lung cancer pretreated with nivolumab: a case report. Mol Clin Oncol 2017; 7: 383-385.

[43] Ekor M. The growing use of herbal medicines: issues relating to adverse reactions and challenges in monitoring safety. Front Pharmacol 2014; 4: 177.